

Resonant band-f scattering and the magnetic properties of highly correlated actinide systems

G.-J. Hu, N. Kioussis, B. R. Cooper, and A. Banerjea

Citation: *Journal of Applied Physics* **61**, 3385 (1987); doi: 10.1063/1.338780

View online: <http://dx.doi.org/10.1063/1.338780>

View Table of Contents: <http://scitation.aip.org/content/aip/journal/jap/61/8?ver=pdfcov>

Published by the [AIP Publishing](#)

Articles you may be interested in

Electronic and magnetic properties of manganite thin films with different compositions and its correlation with transport properties: An X-ray resonant magnetic scattering study

J. Appl. Phys. **116**, 222205 (2014); 10.1063/1.4902959

5f band dispersion in the highly correlated electronic structure of uranium compounds

AIP Conf. Proc. **532**, 420 (2000); 10.1063/1.1292353

A high repetition rate solid state laser system for resonance ionization mass spectrometry of actinides

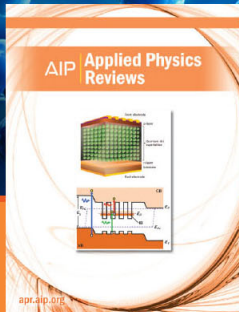
AIP Conf. Proc. **454**, 285 (1998); 10.1063/1.57161

Correlated band magnetism of cerium and actinide materials

J. Appl. Phys. **81**, 3856 (1997); 10.1063/1.364732

Stabilization of the 5f Energy Band in Actinide- Rh 3 Intermetallic Compounds

AIP Conf. Proc. **10**, 1076 (1973); 10.1063/1.2946747



NEW Special Topic Sections

NOW ONLINE
Lithium Niobate Properties and Applications:
Reviews of Emerging Trends

AIP | Applied Physics Reviews

Resonant band- f scattering and the magnetic properties of highly correlated actinide systems

G.-J. Hu, N. Kioussis, and B. R. Cooper

Department of Physics, West Virginia University, Morgantown, West Virginia 26506

A. Banerjee

Department of Physics, West Virginia University, Morgantown, West Virginia 26506 and General Motors Research Laboratory,^{a)} Warren, Michigan 48090

To understand the magnetic properties of moderately delocalized light actinide (uranium, neptunium, plutonium) systems, it is necessary to treat correctly the way in which the highly correlated behavior of the f electrons within the actinide ion is linked to the non- f band behavior via the hybridization process. We do this by transforming the hybridization into band- f resonant scattering. We have successfully applied the theory to PuSb by considering both dominant and next-to-dominant scattering channels.

I. INTRODUCTION

The magnetic behavior of the cerium monopnictides has been understood¹ on the basis of interactions that arise from the hybridization of non- f band electrons with moderately delocalized f electrons. This hybridization was first treated by Coqblin and Schrieffer² by transforming it into band- f resonant scattering from Ce^{3+} (f^1) ions. Extending this theory to the general case of f ions with more than one f electron in each ion, Cooper *et al.*^{1,3-5} reported the results of calculations for the Pu^{3+} (f^5) system in the cases of j - j coupling, L-S coupling, and intermediate coupling. Success was achieved⁵ in explaining the main features^{4,6} of the anisotropic magnetic equilibrium behavior of PuSb, namely, the variation of the magnetization with temperature and phase transition from a ferromagnetic phase to a long-period antiferromagnetic phase; but the theory failed to reproduce the correct polarization (longitudinal to the modulation direction) for the long-period antiferromagnetic structure observed⁶ in the temperature range below the Néel temperature T_N . The theory also gave⁷ a susceptibility singularity in the near-critical region corresponding to the incorrect polarization. For the excitation behavior, the theory failed to explain why for PuSb there are⁸ two modes at the zone boundary for the wave vector perpendicular to the magnetic moment. (These modes are at least partially polarized, parallel and perpendicular to the wave vector, respectively.⁸)

II. RESONANT SCATTERING THEORY AND RESULTS

In the original calculations⁹⁻¹² for Ce^{3+} systems, the dominant contribution to the lowest order in $(k_F R)^{-1}$ to the two-ion interaction came from processes in which the electron involved in the associated single-site scattering event had magnetic quantum number (with respect to the interionic axis) $m_j = \pm 1/2$ ($m_l = 0, m_s = \pm 1/2$); however, some contribution from $m_j = \pm 1/2$ states with $m_l = +1$ was also included. On extending the theory to systems with more than one f electron per ion, Thayamballi and Cooper³ and Banerjee *et al.*⁵ assumed that only one electron (out of the many-electron ionic state) with $m_l = 0$

($m_j = \pm 1/2$) (one-electron component that points its charge density along the interionic axis taken as the axis of quantization) is involved in the scattering events and the quantum numbers of all the other one-electron components remain unchanged. To remove the discrepancies between theory and experiment we recognized⁵ that the $m_j = \pm 1/2$ states with $m_l = \pm 1$, partially included for the Ce^{3+} theory, must play a crucial "fine tuning" role. (These one-electron states "point" their charge densities off the interionic axis.) Therefore, we have now considered contributions to the two-ion interaction from the following three single-site scattering channels:

- (1) $m_l = 0, m_s = \pm 1/2 \leftrightarrow m'_l = 0, m'_s = \pm 1/2$;
- (2) $m_l = 0, m_s = \pm 1/2 \leftrightarrow m'_l = \pm 1, m'_s = \mp 1/2$;
- (3) $m_l = \pm 1, m_s = \mp 1/2 \leftrightarrow m'_l = \pm 1, m'_s = \mp 1/2$.

In the earlier studies^{3,5} the only channel considered was (1), which, in orders of $(k_F R)^{-1}$, is the leading contribution to the two-ion interaction. After including the next two higher-order contributions, arising from channels 2 and 3, in our calculation, we have obtained some striking results.

A. Longitudinal polarization

Figure 1 shows the polarization diagram in the W_1 vs W_2 plane, i.e., shows whether the long-period antiferromagnetic phase has transverse or longitudinal polarization. Here the phenomenologically introduced weighting factor W_1 (W_2) measures the ratio of the magnitude of contribution to the strength of two-ion interaction (range parameters) of channel 2 (3) to that of channel 1. For the L-S coupling case we find that for a wide range of values of W_1 (0.38–1.0) or of W_2 (0.19–1.0) the magnetic behavior of the Pu^{3+} system, corresponding to PuSb, predicted by the theory gives a longitudinally polarized long-period antiferromagnetic phase. However, in the area with $W_1 < 0.38$ and $W_2 < 0.19$ the polarization is transverse. On the critical line, which separates the longitudinal and transverse areas, the antiferromagnetic phase is unpolarized. It is clear to see that at the point $W_1 = 0, W_2 = 0$, which is the case treated in the previous studies,³⁻⁵ the polarization is transverse. Thus the contribu-

^{a)} Present address.

$\text{Pu}^{3+}(f^5)$, L - S coupling
 $W_1: (m_l = 0 \leftrightarrow m_l = \pm 1)$
 $W_2: (m_l = \pm 1 \leftrightarrow m_l = \pm 1)$

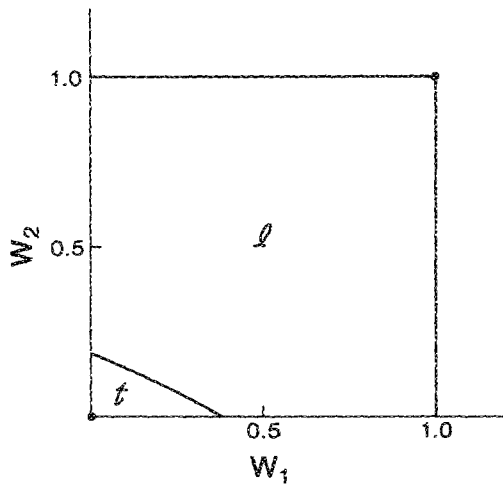


FIG. 1. Polarization behavior as a function of the weighting factors W_1 and W_2 for $\text{Pu}^{3+}(f^5)$ system in the antiferromagnetic phase (in the temperature range below Néel temperature T_N). The longitudinal and transverse polarized phases are labeled by l and t , respectively.

tion of the channels with $m_l = \pm 1$ “tunes” the interaction to provide the experimentally observed polarization in PuSb.

B. Correlation length anisotropy

The ratio $\kappa_{\parallel}/\kappa_{\perp}$ of the inverse critical correlation lengths parallel and perpendicular to moment direction, evaluated at $T - T_N = 0.04T_N$, with negative crystal-field splitting (Γ_8 low) has been calculated for L-S coupling for the case of a longitudinally polarized antiferromagnetic structure with $W_1 = 1$, $W_2 = 0$, $E_2 = E_1$, $E_3 = -0.28E_1$. These parameters provide equilibrium behavior for PuSb closely approximating the experimental behavior. We find that $\kappa_{\parallel}/\kappa_{\perp} \approx 2.2$, and this value is almost independent of the crystal field. The value of $\kappa_{\parallel}/\kappa_{\perp}$ is greater than unity, indicating that the magnetic interactions are stronger within the ferromagnetic planes than are the interplanar couplings. This value of $\kappa_{\parallel}/\kappa_{\perp}$ is in close agreement with that of very recent experiments¹³ giving $\kappa_{\parallel}/\kappa_{\perp} = 1.8 \pm 0.2$ for PuSb. Thus we note two important changes from the previous results⁷ that did not include any contribution from scattering channels (2) and (3) (the $m_l = \pm 1$ channels). The singularity in the near-critical susceptibility now provides the correct polarization as experimentally observed; and the direction of anisotropy for L-S coupling is reversed from that previously found ($\kappa_{\parallel}/\kappa_{\perp} > 1$ as has now been experimentally observed¹³).

C. Two elliptically polarized modes in excitation spectrum

In neutron inelastic scattering experiments Lander *et al.*⁸ recently found a number of interesting features in the excitation spectrum of PuSb in the low-temperature phase. Particularly interesting is that there exist two modes, on ap-

proaching the zone boundary in the transverse direction [100] (the modulation is along [001] direction), and these modes are at least partially linearly polarized (i.e., are at least elliptically rather than circularly polarized). At the zone boundary the mode at 4.3 THz has y polarization (transverse to wave vector) whereas the mode at 3.5 ± 0.2 THz has x polarization (parallel to wave vector). At (0.7,0,0) two separate modes can no longer be distinguished.

The present theory allows us to understand this unusual feature. Figure 2 shows the calculated excitation spectra at $T = 0$ K, for the L - S coupling case with $W_1 = 1$, $W_2 = 0$, $E_2 = E_1$, $E_3 = -0.306E_1$, $60B_4 = -0.38E_1$ ($E_1 = 121.43$ K was chosen to match the experimental Néel temperature, $T_N = 85$ K). Here E_1 , E_2 , E_3 are the range parameters¹ and B_4 is the crystal-field parameter. The crystal-field splitting Δ_{CF} , which is strongly modified¹⁴ by the hybridization, is treated phenomenologically with $\Delta_{CF} = 360B_4$; and a negative B_4 gives a Γ_8 ground state. The solid lines in Fig. 2 show the intense modes which are likely to be observed experimentally. The dominant mode L_{41} has an excitation energy of about 3.4 THz (164 K) at the Γ point and increases in energy as we go toward the X points. At about (0.7,0,0) the mixing of the transverse modes L_{31} and L_{41} starts to occur. This is associated with the reduction of the intensity of the L_{41} mode, with a corresponding increase in the L_{31} mode intensity. This admixture produces two el-

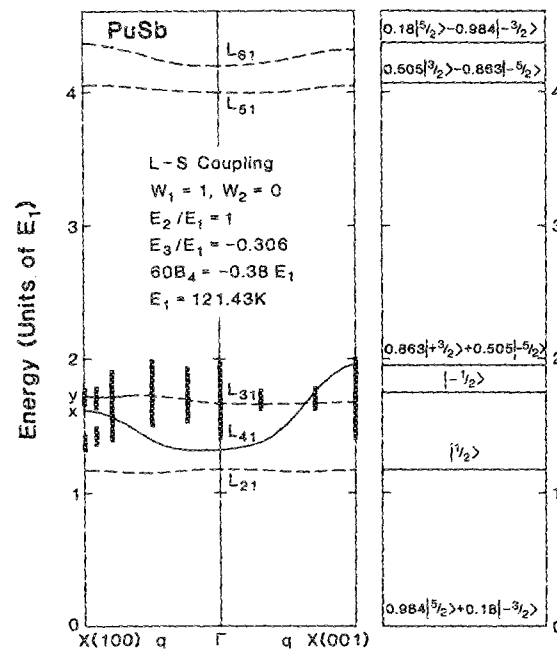


FIG. 2. Dispersion curves for excitations in the ferromagnetic phase at $T = 0$ with L-S coupling, $E_2 = E_1$, $E_3 = 0.306E_1$, and $B_4 = -(0.38/60)E_1$ with weighting $W_1 = 1$, $W_2 = 0$ for q along the [100] and [001] (directions parallel and perpendicular to the moment direction, respectively). $E_1 = 121$ K to match experimental T_N . The solid curves L_{31} near $X(100)$ and L_{41} show the most intense mode. Modes L_{31} , L_{41} , and L_{51} are transverse modes and modes L_{61} and L_{21} are longitudinal and quadrupolar modes, respectively. The energy levels of the molecular-field states and their compositions in terms of the angular momentum eigenstates (quantized along [001]) are shown on the far right. Heavy bars show the experimental results of Lander *et al.* (Ref. 8) for PuSb.

liptically polarized branches: a y -polarized (major axis) upper branch and an x -polarized lower branch. At the zone boundary [$q = (1,0,0)$ direction] the two predicted modes have energies 4.5 THz (216 K) and 4 THz (194 K), respectively, and the polarization ($\langle J_y^2 \rangle / \langle J_x^2 \rangle$)^{1/2} is $\sqrt{2}$ for the upper branch and $(1/\sqrt{6})$ for the lower branch.

The relative separations between modes are quite sensitively dependent on the value of B_4 . To bring modes L_{31} and L_{41} close enough to cause the admixture at the zone boundary (i.e., to give two intense modes) the value of $60B_4$ must be chosen in a narrow range from $-0.35E_1$ to $-0.40E_1$. Outside this range of B_4 the only intense mode is L_{41} , and this is circularly polarized. In fact, we chose B_4 to provide the mode mixing giving two intense (and elliptically polarized) modes at the zone boundary. It is a remarkable result that this choice of crystal-field splitting parameter places the mode energies almost exactly at the experimental values. This result indicates that for PuSb the crystal-field splitting from Γ_8 to Γ_7 should be about 255–290 K. Further experimental information checking this predicted value would be valuable.

We have also carried out calculations for the Pu^{3+} system in the case of intermediate coupling (IC). After a tedious evaluation we found almost the same results as we have obtained in the L-S coupling limit. This is not surprising since the ground state of the L-S coupling limit is the predominant component of the IC ground state which we take as 75% 6H and 25% 4G .

One discrepancy exists between the calculated and observed excitation behavior at low temperature. While the experimentally observed magnetic transition is almost dispersionless for q along the $[001]$ direction, and a clearly defined minimum occurs for the low-energy branch at the zone boundary (X point), our theory predicts that the intense mode has significant dispersion for q along both the $[001]$ and $[100]$ directions with an energy minimum at the Γ point regardless of the choice of phenomenological parameters.

In conclusion, we have found that upon including the additional (next-to-dominant) channels for the single-site

scattering events the hybridization-mediated interaction fully explains the anisotropic magnetic equilibrium behavior for the Pu^{3+} (f^5) system. The longitudinally polarized anti-ferromagnetic phase has been satisfactorily obtained by considering the contribution of the additional scattering channels, which is equivalent to including off-axis f -electron charge distribution. We also obtain excellent agreement with experiment¹³ for the correlation length anisotropy. The theory also gives a magnetic excitation spectrum at $T = 0$ in the ferromagnetic phase with two polarized branches at the zone boundary with q along the $[100]$ (transverse to moment) direction. The predicted crystal-field splitting from Γ_8 to Γ_7 is about 255–290 K.

ACKNOWLEDGMENT

This research has been supported by the U.S. Department of Energy through Grant DE-FG05-84-ER45134.

¹B. R. Cooper, R. Siemann, D. Yang, P. Thayamballi, and A. Banerjea, *Handbook on the Physics and Chemistry of the Actinides*, edited by A. J. Freeman and G. H. Lander (North-Holland, Amsterdam, 1985), Vol. 2, Chap. 6, pp. 435–500.

²B. Coqblin and J. R. Schrieffer, *Phys. Rev.* **285**, 847 (1969).

³P. Thayamballi and B. R. Cooper, *J. Appl. Phys.* **55**, 1829 (1984).

⁴B. R. Cooper, P. Thayamballi, J. C. Spirlet, W. Müller, and O. Vogt, *Phys. Rev. Lett.* **51**, 2418 (1985).

⁵A. Banerjea, B. R. Cooper, and P. Thayamballi, *Phys. Rev. B* **30**, 2671 (1984); A. Banerjea and B. R. Cooper, *Phys. Rev. B* **34**, 1607 (1986).

⁶P. Burllet, S. Quezel, J. Rossat-Mignod, J. C. Spirlet, J. Rebizant, W. Müller, and O. Vogt, *Phys. Rev. B* **30**, 6660 (1984).

⁷N. Kioussis and B. R. Cooper, *Phys. Rev. B* **34**, 3261 (1986).

⁸G. H. Lander, W. G. Stirling, J. Rossat-Mignod, J. C. Spirlet, J. Rebizant, and O. Vogt, *Physica* **136B**, 409 (1986).

⁹R. Siemann and B. R. Cooper, *Phys. Rev. Lett.* **44**, 1015 (1980).

¹⁰B. R. Cooper, *J. Magn. Magn. Mater.* **29**, 230 (1982).

¹¹D. Yang and B. R. Cooper, *J. Appl. Phys.* **53**, 1988 (1982).

¹²B. R. Cooper, P. Thayamballi, and D. Yang, *J. Appl. Phys.* **55**, 1866 (1984); P. Thayamballi, D. Yang, and B. R. Cooper, *Phys. Rev. B* **29**, 4049 (1984).

¹³P. Burllet, J. Rossat-Mignod, G. H. Lander, J. C. Spirlet, J. Rebizant, and O. Vogt, *Phys. Rev. B* (to be published).

¹⁴J. M. Wills, B. R. Cooper, and P. Thayamballi, *J. Appl. Phys.* **57**, 3183 (1985).